ASTRONOMY & ASTROPHYSICS
SUPPLEMENT SERIES

Astron. Astrophys. Suppl. Ser. **136**, 227–235 (1999)

The 3-D structure of the Coma–A 1367 supercluster: Optical spectroscopy of 102 galaxies⋆

G. Gavazzi[1], **L. Carrasco**[2,3], **and R. Galli**[1]

[1] Universitá degli Studi di Milano, Via Celoria 16, 20133 Milano, Italy
[2] Instituto Nacional de Astrofísica, Optica y Electrónica, Apartado Postal 51, C.P. 72000 Puebla, Pue., Mexico
[3] Observatorio Astronómico Nacional/UNAM, Ensenada B.C., Mexico

Received July 3; accepted October 2, 1998

Abstract. Optical spectroscopy of 117 CGCG galaxies, 102 of which are projected in the direction of the Coma–A 1367 supercluster, is reported. These new measurements, added to those found in the literature, bring to 1068 the number of CGCG galaxies in this region with available redshift, out of a total of 1085 objects with $m_{\rm p} \leq 15.7$. We use these data to infer the 3-D structure of the Coma supercluster.

Key words: galaxies: redshift — galaxies: clusters: Coma; A 1367

1. Introduction

The Coma–A 1367 supercluster is part of the Great Wall, the major large-scale structure in the Northern Hemisphere (Zabludoff et al. 1993). This supercluster provides us with a unique test-bed for extragalactic investigations since it contains thousands relatively bright galaxies ($m_{\rm p} < 15.7$) at high galactic latitude, thus little affected by extinction from our Galaxy, distributed in a variety of environments spanning from rich clusters (Coma + A 1367) to relatively low-density regions. Furthermore, due to its narrow distribution in the redshift space relative to its average recessional velocity (7000 $\mathrm{km\,s^{-1}}$), the distance spread of its members is minimal. These properties make the Coma supercluster ideal for studying the environmental dependence of the properties of galaxies (e.g. their luminosity function) spanning a local density regime of over an order of magnitude. This structure has been studied in increasing details in the last decades, as new redshift measurements became available. The pioneering work of Gregory & Thompson (1978) unveiled the main structure of the supercluster within the region $11^{\rm h}30^{\rm m} < \alpha < 13^{\rm h}30^{\rm m}; 18^\circ < \delta < 32^\circ$. By that time only 238 of the 1130 galaxies brighter than 15.7 catalogued in the CGCG (Zwicky et al. 1961-68) in this region, had known redshift values. Ten years later the analysis of Gavazzi (1987) counted more than twice as many velocity measurements (695) obtained from optical (de Lapparent et al. 1986; Huchra et al. 1990) and 21 cm spectra (Giovanelli & Haynes 1985). The recent determination of the luminosity function of galaxies in this region by Gavazzi et al. (1995) relied on 941 redshifts. However complete optical and near-IR photometry was available for the late-type population only (Gavazzi & Boselli 1996). Since then the photometric survey was extended to cover the early-type galaxies as well, at least in the near-IR (Gavazzi et al. in preparation), while measurements in the visible are still under way. The full exploitation of this photometric material requires extending the redshift survey to the remaining 189 unmeasured galaxies. For this purpose we undertook the spectroscopic survey presented in this paper. The sample is presented in Sect. 2, the observations and data reduction in Sect. 3. The new redshift are given in Sect. 4 and are used, joint with the measurements from the literature, to study the 3-D structure of the Coma supercluster.

2. The sample

Galaxies in the present study are selected from the CGCG Catalogue (Zwicky et al. 1961-68) in the region $11^{\rm h}30^{\rm m} < \alpha < 13^{\rm h}30^{\rm m}; 18^\circ < \delta < 32^\circ$ containing the Coma–A 1367 supercluster. There are 1130 galaxies listed in this region. Of these 1085 have $m_{\rm p} \leq 15.7$. Another 45 belong to multiple systems which were split in their individual components, each of them fainter than the catalogue limiting magnitude 15.7. Out of the 1130 we observed 102 galaxies

Send offprint requests to: gavazzi@uni.mi.astro.it

⋆ Based on observations obtained with the Loiano telescope belonging to the University of Bologna, Italy, and with the G. Haro telescope of the INAOE, Mexico.

Table 1. The spectrograph characteristics

Tel	Spectrog.	dispersion Å/mm	coverage Å	CCD type	pix μm
Loiano	BFOSC	198	$4060-7900$	1024×1024 TH	19
Cananea	LFOSC	228	$4000-7100$	576×384 TH	23

with no z values available in the literature. Only 17/1085 galaxies with $m_{\rm p}\leq15.7$ in the Coma region and 45/1130 fainter than this limit remain with unknown redshift, thus the sample is 98% complete at 15.7. Spectra of 3 galaxies belonging to the cluster A 262 and 12 to the Hercules supercluster were also taken as fillers.

3. Observations and data reduction

Low dispersion spectra of 117 galaxies were obtained in several observing runs since 1995 using the imaging spectrographs BFOSC and LFOSC attached to the Cassini 1.5 m telescope (Loi) at Loiano (Italy) and the 2.1 m telescope (Can) of the Guillermo Haro Observatory at Cananea (Mexico), respectively.

Table 1 lists the characteristics of the two spectrographs in the adopted configurations:

The observations at Loiano were performed using a 2.0 or 2.5 arcsec slit, depending on the seeing conditions, oriented E-W. The exposure time ranged between 20 and 90 min according to the brightness of the target object. Observations at Cananea were carried out with a 3.1 arcsec fixed slit, oriented N-S. Every galaxy spectrum was preceded and followed by an exposure of a HeAr lamp (Loiano) or XeNe lamp (Cananea) to secure the wavelength calibration.

Data reduction was performed in the IRAF-PROS environment. After bias subtraction, when 3 or more frames of the same target were obtained, these were combined (after spatial alignment) using a median filter to help cosmic rays removal. Otherwise the cosmic rays were removed under visual inspection. The wavelength calibration was checked on known sky lines. These were found within ~1 Å from their nominal value, providing an estimate of the systematic uncertainty on the derived velocities of ~50 km s^{-1}. After subtraction of the sky background, one-dimensional spectra were extracted from the frames. These spectra were analyzed with either of two methods:

1) **individual line measurement**: all spectra taken at Cananea and those obtained at Loiano prior to 1996 were inspected and emission/absorption lines were identified. Emission lines include Hα, N[II] and S[II]. Absorption lines include the Mg[I], CaFe and Na. The galaxy redshift was obtained from these individual measurements. If more than one line was identified, the galaxy redshift was derived as the weighted mean of the individual measurements, with weights proportional to the line intensities.

2) **Cross correlation technique**: spectra obtained at Loiano after 1996 were analyzed using the cross-correlation technique of Tonry & Davis (1979). This method is based on a "comparison" between the spectrum of a galaxy whose redshift is to be determined, and a fiducial spectral template of a galaxy (or star) of appropriate spectral type to contain the wanted absorption/emission lines. The basic assumption behind this method is that the spectrum of a galaxy is well approximated by the spectrum of its stars, modified by the effects of the stellar motions inside the galaxy and by the systemic redshift. For this purpose high signal-to-noise spectra were taken of two template galaxies: M105 (absorption lines) and NGC 1330 (emission lines), whose redshifts are 866 and 1039 km s^{-1} respectively.

The observed redshifts ($V_{\rm obs}$) were first transformed to Heliocentric ($V_{\rm hel}$), then corrected for the motion of our galaxy relative to the Cosmic Microwave Background ($V_{\rm CMB}$) according to Kogut et al. (1993).

4. Results

The velocity measurements obtained in this work are listed in Table 2 as follow:
Column 1: the CGCG designation (Zwicky et al. 1961-68).
Columns 2, 3: (B1950) celestial coordinates, measured with few arcsec uncertainty.
Column 4: the photographic magnitude (Zwicky et al. 1961-68).
Columns 5, 6: the derived heliocentric velocity with uncertainty. The latter quantity is obtained by adding in quadrature systematic and statistical errors.
Column 7: an asterisk marks uncertain redshifts. These are either low signal spectra or spectra with only one absorption line that could be misidentified.
Column 8: type of lines (A = absorption; E = emission; EA = both).
Column 9: method used for the redshift measurement (CC = cross correlation; IL = individual line measurement).
Column 10: observing run.

Figure 1 gives a representation in celestial coordinates of 1085 galaxies (panel a) and a wedge diagram ($V_{\rm CMB}$ vs. R.A.) is given in panel b. Small symbols mark galaxies

Table 2. Parameters of the observed galaxies

CGCG	RA(1950) h m s	Dec(1950) ° ′ ″	m_p mag	V_{hel} km s^{-1}	±	Qual.	Lines	Method	run
(1)	(2)	(3)	(4)	(5)	(6)	(7)	(8)	(9)	(10)
522029 S	014918.79	345434.5	15.6	25277	221		E	CC	L97
522029 N	014920.02	345454.9	16.5	25638	127	*	E	CC	L97
522034 S	014941.55	355241.4	15.0	4382	318		A	IL	L95
97007	113029.29	200048.8	15.5	10138	147		EA	IL	L95
97009	113036.57	200527.5	15.6	9936	147		EA	IL	L95
97011	113113.56	201803.2	15.6	10475	136		EA	IL	C97
97013	113158.13	185729.8	15.6	3283	172		E	IL	C97
97035	113600.31	180558.3	15.2	18562	84		E	IL	L96
97036	113614.86	195243.0	15.7	6595	71		E	IL	C97
97037	113631.60	193825.3	15.6	10811	336		A	IL	C97
127020	113709.54	252835.1	15.6	3690	183		EA	IL	C95
127019	113711.80	234833.2	15.6	9246	147		A	IL	L95
97046	113718.28	180931.7	15.7	22800	172	*	A	IL	C97
127023	113733.62	253513.4	15.4	6682	311		A	CC	L97
127021	113735.53	234755.7	15.7	9939	71		A	IL	C97
97053	113750.29	194128.7	15.7	3079	172		E	IL	C97
97066	113950.99	180218.1	15.7	10388	147		E	IL	L95
97069	113956.11	180342.7	15.6	10523	147		E	IL	L95
157019	114016.06	264903.6	15.6	8486	81		A	IL	C95
97076	114026.46	195539.0	15.5	7060	346	*	A	IL	L96
127041	114108.44	254406.9	15.5	14713	70		E	CC	L97
97102 S	114140.80	202940.4	15.5	6445	243		A	CC	L97
97111 S	114150.40	202249.8	16.5	7239	448		A	CC	L97
127043	114158.25	254155.6	15.0	13323	147	*	A	IL	L95
127044	114212.56	241259.8	15.6	9917	250		A	CC	L97
97136	114307.32	180132.3	15.4	6238	216		A	CC	L97
97154	114527.86	185539.5	15.7	12165	375		A	IL	C97
127057	114550.12	260244.3	15.7	13212	140		E	IL	C97
127066	114745.63	221727.0	15.6	10315	64		E	IL	C95
97160	114758.48	180811.1	15.6	6025	75		E	IL	C97
97162	114815.78	201936.2	15.7	6212	172		A	IL	C97
127069	114816.25	214002.4	15.7	7960	258		A	IL	C97
127077	114856.25	240826.2	15.1	7057	227	*	A	IL	L96
97168	114913.57	193812.3	15.7	5996	172		E	IL	C97
97172	114939.64	185547.2	15.7	7650	56		E	IL	C97
97173	115006.63	202531.7	15.7	14874	330		A	IL	C97
127093	115036.00	254258.6	15.1	13250	154	*	EA	IL	L95
97176	115115.54	200142.9	15.5	12056	263		A	CC	L97
98001	115125.40	201409.0	15.6	15489	90		E	CC	L97
127105	115256.37	251321.1	15.7	8450	66		E	IL	C97
98005	115301.87	181825.7	15.5	16263	430	*	A	CC	L97
98010	115440.93	183443.5	15.7	23407	71	*	EA	IL	C97
127113	115517.04	223211.4	15.5	9219	590	*	A	CC	L97
127121	115551.31	252233.7	15.7	4131	172	*	E	IL	C97
98014	115608.82	192530.9	15.7	13420	137		A	IL	C97
127128 N	115653.81	211720.8	15.7	7147	60		E	IL	C97
127129	115655.62	254450.5	15.5	13594	348		A	CC	L97
127131	115710.12	255359.0	15.7	17490	204		A	IL	C97
127132	115751.36	215012.9	15.6	14609	147		A	IL	L95

Table 2. continued

CGCG	RA(1950) h m s	Dec(1950) ° ′ ″	m_p mag	V_{hel} km s^{-1}	±	Qual.	Lines	Method	run
(1)	(2)	(3)	(4)	(5)	(6)	(7)	(8)	(9)	(10)
98018	115801.76	181752.7	15.7	6959	172	*	E	IL	C97
127134	115838.73	225342.5	15.7	8439	110		E	IL	C97
98023	115910.69	181036.1	15.1	6920	81		EA	IL	L95
127138	115921.82	210134.4	15.5	7210	339	*	A	CC	L97
127137 E	115923.50	204057.7	15.6	22478	198		A	IL	C97
98026	115931.25	181127.1	15.6	6764	140		EA	IL	C97
98028	115931.81	180603.3	15.0	6888	115		A	IL	L96
127140	115937.08	243440.5	15.7	13361	636	*	A	IL	C97
127141	115952.75	240548.8	15.0	6700	145		A	IL	L96
128001	120003.94	212618.1	15.5	7489	206		A	CC	L97
128006	120127.50	203656.6	15.6	6719	100		A	IL	C97
98045	120140.37	202917.1	15.6	6375	125		A	IL	C97
128011	120143.20	242518.0	15.7	15073	160	*	A	IL	C97
98048	120217.37	193134.0	15.2	6944	206		A	IL	L96
128015	120222.87	213109.7	15.3	6832	147		E	IL	L95
128019	120254.50	203511.9	15.0	7289	224		EA	IL	L96
128018	120256.06	203130.7	15.1	7257	137		A	IL	L96
128020	120304.19	205001.9	14.9	7155	140		A	IL	L96
128022	120307.00	205002.3	15.2	7580	71	*	A	IL	L96
128024	120318.31	204759.0	15.3	7268	316		A	CC	L97
98054	120344.04	182850.2	15.6	6868	239		A	IL	C97
98067	120607.30	181404.4	15.7	7610	172		E	IL	C97
98068	120633.95	202705.2	15.7	19324	976		A	IL	C97
98072	120658.36	192915.9	15.7	7946	172		E	IL	C97
98074	120725.28	201146.0	15.6	7471	147		E	IL	L95
98075	120732.92	202931.7	15.7	24934	172	*	A	IL	C97
98076	120741.87	192818.1	15.5	7804	385		A	CC	L97
98081	120809.37	180955.8	15.2	7177	132		EA	IL	L95
98082	120812.94	191907.8	14.7	7454	76		A	IL	L96
98087	120849.31	192200.4	15.3	7540	122		A	IL	L95
98090	120905.37	200724.7	15.7	6537	99		E	CC	L98
98091	120911.77	194606.1	15.6	3350	92		E	CC	L98
98104	121045.94	201249.3	15.6	8349	147		E	IL	L95
98112	121135.86	193650.2	15.6	15198	400		A	CC	L97
128057	121150.34	222755.4	15.6	6998	174	*	E	CC	L97
98121	121343.01	180441.8	15.4	9000	153		E	IL	L95
98122	121344.64	184125.4	15.7	8968	125		E	CC	L98
99002	121523.76	184037.5	15.5	7681	108		E	CC	L97
128072	121536.82	245758.1	15.4	6866	69		E	IL	C95
99004	121543.32	201717.4	15.6	8744	138		E	IL	C95
99006	121552.00	202510.2	15.5	8516	94		E	CC	L97
99009	121609.64	182819.2	15.6	9358	166		E	CC	L98
128076	121717.15	210706.0	15.7	9359	78		E	CC	L98
128086	122227.12	243933.5	15.6	10245	311	*	EA	CC	L98
128088	122337.28	203646.4	15.7	9361	385	*	A	CC	L98
128091	122601.19	233452.2	15.3	6639	278		A	CC	L97

taken from the literature, filled circles mark the measurements obtained in this work.

Figure 2 gives a histogram of the galaxy velocity distribution (panel a). The present measurements are given in a separate histogram (panel b). Since, for obvious reasons, we measured galaxies fainter than average, the fraction of background objects (panel c) is higher than in the general sample. However, even at the present limiting magnitude, nearly 50% of the new redshifts are found in the range $6000 - 8500$ km s^{-1}, typical of the Coma supercluster.

4.1. The 3-D structure of the Coma–A 1367 supercluster

The aim of this work is to try an objective determination of the "aggregation" state of galaxies in the

Table 2. continued

CGCG	RA(1950) h m s	Dec(1950) ° ′ ″	m_p mag	V_{hel} km s^{-1}	±	Qual.	Lines	Method	run
(1)	(2)	(3)	(4)	(5)	(6)	(7)	(8)	(9)	(10)
99064	122605.12	194449.1	15.2	13497	203		EA	IL	L95
129004	122719.12	223853.9	15.2	6847	71		E	IL	L95
99070	122756.34	190508.5	15.4	14575	155		E	CC	L97
99071	122759.12	195658.3	15.0	885	197	*	A	CC	L97
129006	122911.59	204525.8	15.6	1921	55		E	IL	C95
129007	123232.27	260318.0	15.7	8673	114		E	IL	C97
159049 S	123756.90	264641.0	15.7	6330	172		A	IL	C97
159049 N	123757.20	264755.0	15.4	7280	132	*	E	IL	C97
161050	132402.10	315731.0	15.6	14989	136		E	CC	L98
161061 S	132554.00	285542.1	15.6	11247	71		E	IL	C95
108024	155546.36	152733.6	15.6	11070	156		EA	IL	C97
108025	155605.62	181322.0	15.6	13481	74		A	IL	C97
108032	155647.22	195309.8	15.6	5488	74		E	IL	L96
108040	155807.52	193451.4	15.7	13817	147		E	IL	L96
108052	155842.70	184514.5	15.7	10649	171		A	IL	C97
108077	160013.97	144134.3	15.7	10279	100		A	IL	C97
108080	160034.69	195530.1	15.7	1663	188	*	A	IL	C97
108090	160137.46	150218.2	15.6	10779	113		A	IL	C97
108103	160227.38	163925.9	15.6	13418	147		EA	IL	C97
108114	160303.88	155219.7	15.7	10723	94		E	IL	L96
108125	160319.47	163936.0	15.6	4603	56		E	IL	C97
224037 S	162647.90	411609.6	15.5	9489	72		A	IL	C97

Coma–A 1367 supercluster, i.e. to establish the membership of galaxies to structures of a given size and complexity (e.g. clusters, groups, multiplets etc.) or their degree of "isolation". This is not a trivial exercise since this definition depends on two arbitrary quantities: the scale on which the local density is computed and the local density itself. Consider for example a pair of galaxies with a separation of say 100 kpc. This doublet could be relatively isolated in space, or embedded in a group of galaxies, or in a much larger cluster containing hundreds of galaxies. These three cases, in spite of their similar local densities (i.e. computed on 100 kpc radius), are subject to extremely different environmental conditions: the first (isolated pair) is dominated by the gravitational (tidal) force induced by its companion, whereas in the second example the prevailing conditions are dictated by the group potential and in the third by the large-scale cluster potential or might be severely influenced by the diffuse intracluster gas (e.g. ram pressure). These prevailing environmental conditions are thus "described" by a density parameter which must be computed within a radius similar to the typical scale of the aggregate. Once the densities are computed, these can be converted into (mutually exclusive) "aggregation" classes using appropriate density thresholds.

4.2. The 3-D algorithm

The structure of the Coma–A 1367 supercluster stands out clearly in Figs. 1 and 2 as the pronounced density enhancement centered at 7200 km s^{-1}, stretching through the entire R.A. window. Conspicuous features are: the "fingers of god" of the two clusters Coma and A 1367 which span the interval $4000 < V < 10000$ km s^{-1} and the large "void" in front of the supercluster. The remaining objects, belonging to the bridge between the two clusters have a narrower velocity distribution, which lies within the interval of roughly $6000 < V < 8500$ km s^{-1}.

To reconstruct the 3-D structure of the supercluster we proceed as follows:

1) **Clusters** (Agg = 1 to 4): we identify the members of the two rich clusters using a preliminary conservative positional criterion: in the velocity range $4000 < V < 10000$ km s^{-1} there are 72 galaxies within 1 deg radius (Agg = 1) and 177 within 2 deg (Agg = 2) of the Coma cluster and 59 galaxies within 0.5 (Agg = 3.0) and 81 within 1 deg radius of A 1367 (Agg = 4.0). We subtract these objects from the sample.

2) **"Homunculus"** (Agg = 16): we identify on a purely positional basis the members of the "legs of the homunculus" (see de Lapparent et al. 1986) (Agg = 16) and we subtract these objects from the sample.

3) **Foreground** (Agg = 8 to 18): we subtract from the remaining sample all galaxies with $V < 6000$ km s^{-1}, which are considered as foreground objects. These are empirically assigned to individual groups and structures on the basis of their 3-D coordinates (Agg = 8 to 18 as defined

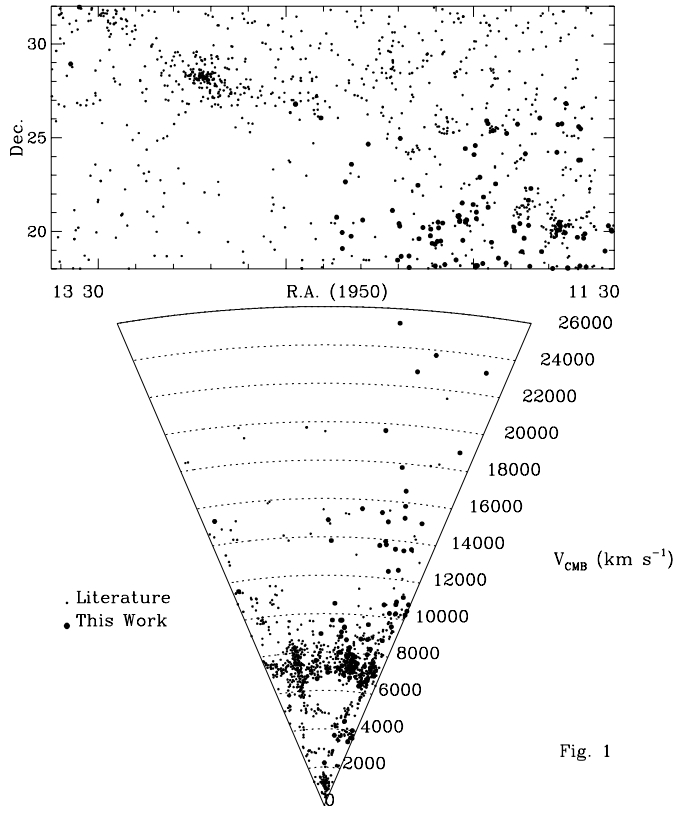

Fig. 1. The distribution in celestial coordinates of 1085 galaxies in the direction of the Coma–A 1367 supercluster, panel **a)**. A wedge diagram ($V_{\rm CMB}$ vs. R.A.) is given in panel **b)**. Small symbols mark galaxies taken from the literature, filled circles mark the measurements obtained in this work

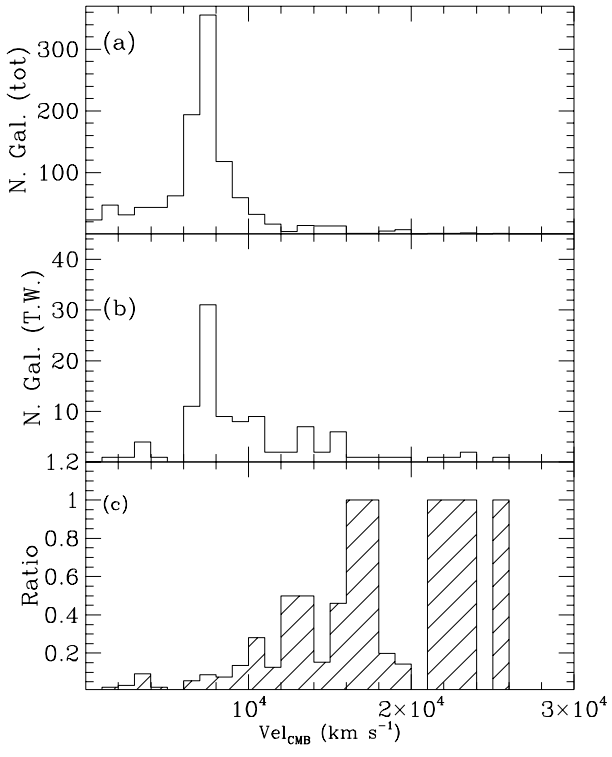

Fig. 2. Velocity histogram of the 1085 available redshifts, panel **a)**, of the 102 redshifts obtained in this work, panel **b)** and of the ratio of new to all redshifts, panel **c)**

in Gavazzi 1987) (see Table 3 below for details). Figure 3 gives a representation in celestial coordinates of the foreground galaxies (including Agg = 16) panel a) and a wedge diagram ($V_{\rm CMB}$ vs. R.A.) is given in panel b.

4) **Background** (Agg = 19.0): we subtract from the remaining sample all galaxies with $V > 8600$ km s^{-1}, which are considered as background objects.

5) **Groups** (Agg = 5.): on the remaining sample ($6000 < V < 8600$ km s^{-1}) we run an algorithm that counts around each galaxy the number of galaxies found within 0.9 Mpc projected radius, satisfying the additional requirement that their velocity is within 600 km s^{-1} from the mean velocity of the aggregate under study (850 km s^{-1} for group 5.3). If there are at least 8 such galaxies, these are assigned to the "group" class (Agg = 5). 5 groups are found by the algorithm (N3937, N4065, IC 762, N4213 and IC 3165) (see Table 3 for details). Figure 4 gives a representation in celestial coordinates of the groups members (panel a) and a wedge diagram is given in panel b. Different symbols are used for the various groups.

6) **Multiplets** (Agg = 6.2 to 6.5): on the remaining sample ($6000 < V < 8600$ km s^{-1}) we run an algorithm that counts around each galaxy the number of galaxies found within 0.3 Mpc projected radius satisfying the additional requirement that their velocity is within 600 km s^{-1} from the mean velocity of the aggregate under study. If there is at least 1 such galaxy, these are assigned to the "multiplet" class (Agg = 6). (6.2 = doublets, 6.3 = triplets... 6.5 = quintuplets).

7) **Contact multiplets** (Agg = 6.1): we repeat 6) with a more stringent requirement that the companion galaxy lies within 50 kpc. these are contact doublets and triplets. Figure 5 gives a representation in celestial coordinates of the members to multiplets (panel a) and a wedge diagram is given in panel b.

8) **Isolated** (Agg = 7.0): on the restricted velocity range $6000 < V < 8000$ km s^{-1} we count galaxies which do not have a companion within 0.3 Mpc projected radius. We call these isolated (Agg = 7.0).

9) **Strictly isolated** (Agg = 7.1) we repeat 8) with the more stringent requirement that the galaxy under study is isolated within 0.5 Mpc projected radius. Figure 6 gives a representation in celestial coordinates of the isolated objects (panel a) and a wedge diagram is given in panel b.

10) **Extended clusters**: finally we re-inject in the sample the cluster objects (see step 1) and try an alternative, less restrictive definition of cluster membership, which

Table 3. The criteria used to define each "Aggregate" in the direction of the Coma–A 1367 supercluster

Agg	Description	N	R/θ Mpc/deg.	R.A. h m	Dec. ° ′	Δ_V km s^{-1}	$V_{\rm min} - V_{\rm max}$ km s^{-1}	$< V >$ km s^{-1}	N
(1)	(2)	(3)	(4)	(5)	(6)	(7)	(8)	(9)	(10)
1.0	Coma Core	–	$\theta < 0.5$	12 57	28 15	2700	4000 – 10000	7145	72
2.0	Coma	–	$0.5 < \theta < 2$	12 57	28 15	1500	4000 – 10000	7244	105
	Coma ext.	> 19	$R < 2$	12 22 – 13 00	26 – 30	1500	4000 – 10000	–	37
3.0	A 1367 Core	–	$\theta < 0.5$	11 42	20 06	2500	4000 – 10000	6805	59
4.0	A 1367	–	$0.5 < \theta < 1$	11 42	20 06	1500	4000 – 10000	6967	22
	A 1367 ext.	> 19	$R < 2$	11 30 – 11 55	19 – 23	1500	4000 – 10000	–	40
5.2	Group N3937	> 8	$R < 0.9$	11 50	20 55	600	6000 – 8600	7002	21
5.3	Group N4065	> 8	$R < 0.9$	12 01	20 30	850	6000 – 8600	7307	25
5.4	Group IC762	> 8	$R < 0.9$	12 05	26 02	600	6000 – 8600	7207	13
5.5	Group N4213	> 8	$R < 0.9$	12 13	24 15	600	6000 – 8600	7054	10
5.6	Group IC3165	> 8	$R < 0.9$	12 17	28 15	600	6000 – 8600	8102	4
6.1	Contact mult.	> 1	$R < 0.05$	11 30 – 13 30	18 – 32	600	6000 – 8600	–	26
6.2	Doublets	1	$R < 0.3$	11 30 – 13 30	18 – 32	600	6000 – 8600	–	55
6.3	Triplets	2	$R < 0.3$	11 30 – 13 30	18 – 32	600	6000 – 8600	–	23
6.4	Quadruplets	3	$R < 0.3$	11 30 – 13 30	18 – 32	600	6000 – 8600	–	9
6.5	Quintuplets	4	$R < 0.3$	11 30 – 13 30	18 – 32	600	6000 – 8600	–	1
7.0	Isolated	0	$R < 0.3$	11 30 – 13 30	18 – 32	–	6000 – 8000	–	75
7.1	Stric. Isolated	0	$R < 0.5$	11 30 – 13 30	18 – 32	–	6000 – 8000	–	122
19.0	Background	–	–	11 30 – 13 30	18 – 32	–	8000–	–	219
8.0	Foreg. Gr. N3798	–	–	11 30 – 11 43	24 – 32	–	3000 – 4000	3883	5
9.0	Foreg. Gr. N3801	–	–	11 30 – 11 43	18 – 24	–	3000 – 4000	3671	13
10.0	Foreg. Gr. N3995	–	–	11 43 – 12 09	18 – 32	–	3000 – 4000	3691	21
11.0	Foreg. Gr. N4005	–	–	11 45 – 12 00	22 – 32	–	4000 – 5500	4864	20
12.0	Foreg. Gr. IC202	–	–	11 46 – 12 14	18 – 22	–	4500 – 5500	4803	3
13.0	Foreg. Gr. N4169	–	–	12 00 – 12 20	26 – 32	–	3500 – 4500	4210	13
14.0	Foreg. Gr. N4615	–	–	12 14 – 12 50	24 – 32	–	4500 – 5700	4996	14
15.0	Foreg. Gr. U8248	–	–	13 03 – 13 30	18 – 26	–	3500 – 4500	4057	7
16.0	Foreg. Gr. N5056	–	–	13 03 – 13 30	28 – 32	–	5000 – 6700	5885	25
17.0	Foreg. Gr. N4794	–	–	11 30 – 13 30	18 – 32	–	2300 – 3200	2813	24
18.0	Foreg. Gr. C1cl.	–	–	11 30 – 13 30	18 – 32	–	0 – 2200	1237	79
19.1	$z = 0$	–	–	11 30 – 13 30	18 – 32	–	– –	–	45

includes more peripheral objects. We count around each galaxy, in the interval $4000 < V < 10000$ km s^{-1}, the number of galaxies found within 2.0 Mpc projected radius. Within $2 < R < 8.5$ deg of the center of Coma and $1 < R < 3.5$ deg of the center of A 367 we allow for a velocity difference of 1500 km s^{-1} from the mean velocity of the cluster. In both aggregates we consider a galaxy to belong to the "extended cluster" if there are >20 galaxies satisfying the above criterion. Figure 7 gives a representation in celestial coordinates of the cluster members (panel a) and a wedge diagram is given in panel b. Different symbols are used for the core, outskirt and extended cluster members.

Figure 8 gives a representation in celestial coordinates of the supercluster members (panel a) and a wedge diagram is given in panel b.

All the above aggregation classes (1-19) are mutually exclusive, except the definition of extended cluster. A galaxy belonging to the extended cluster can be previously defined as belonging to a group, multiplet or even be considered isolated.

The criteria used above are summarized in Table 3 as follows: For any Agg class (Col. 1) a decription is given in Col. 2.

Column 3: the minimum number of objects used to compute the threshold density of each aggregate.

Column 4: the scale (R in Mpc; θ in degrees) used to compute the threshold density of each aggregate.

Columns 5, 6: the "window" in celestial coordinates where each aggregate was found. A single coordinate gives the center of the aggregate (with radius R or θ). If a pair of coordinates is given this indicates the interval where the aggregate was found.

Column 7: the allowed velocity difference from the average velocity of the aggregate.

Columns 8, 9: the velocity interval where the aggregate was found.

Column 10: the average velocity of the aggregate.

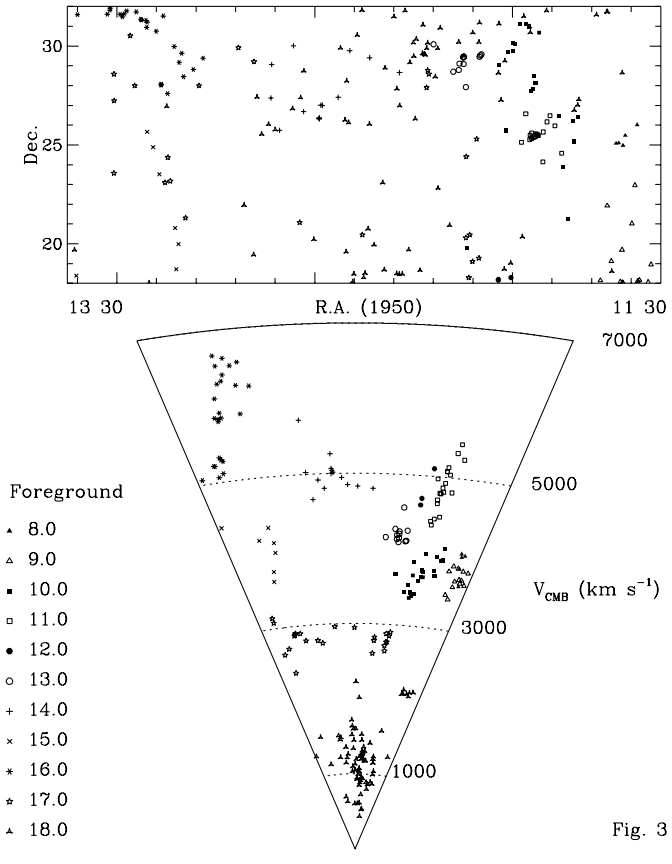

Fig. 3

Fig. 3. The distribution in celestial coordinates of galaxies in the foreground (Agg = 8–18) of the Coma–A 1367 supercluster, panel **a)**. A wedge diagram is given in panel **b)**

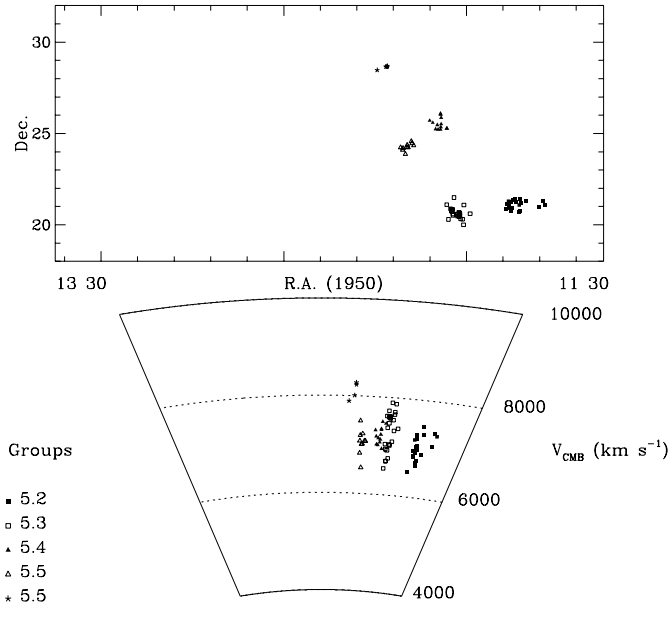

Fig. 4

Fig. 4. The distribution in celestial coordinates of galaxies belonging to 5 groups (Agg = 5) in the Coma–A 1367 supercluster, panel **a)**. A wedge diagram is given in panel **b)**

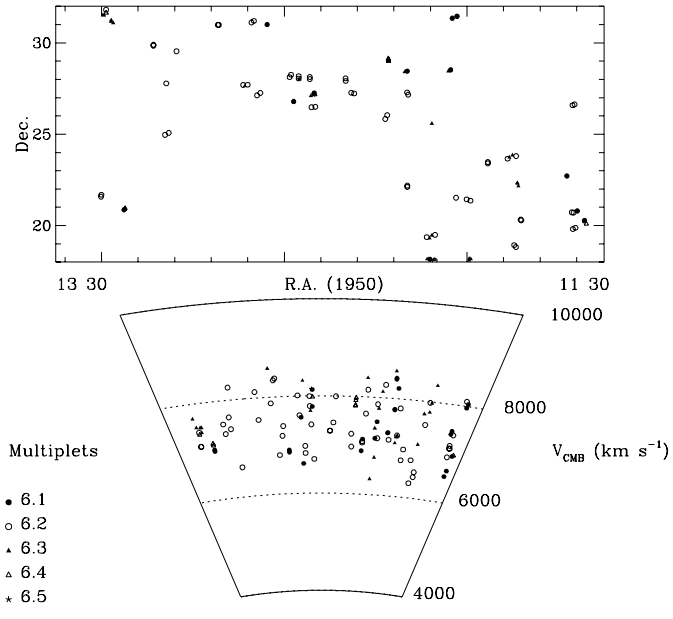

Fig. 5

Fig. 5. The distribution in celestial coordinates of galaxies belonging to multiplets (Agg = 6) in the Coma–A 1367 supercluster, panel **a)**. A wedge diagram is given in panel **b)**

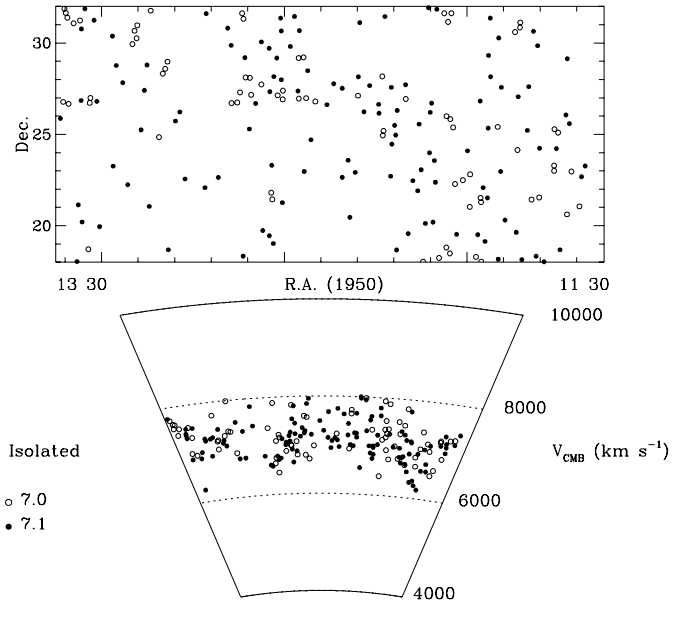

Fig. 6

Fig. 6. The distribution in celestial coordinates of isolated galaxies (Agg = 7) in the Coma–A 1367 supercluster, panel **a)**. A wedge diagram is given in panel **b)**

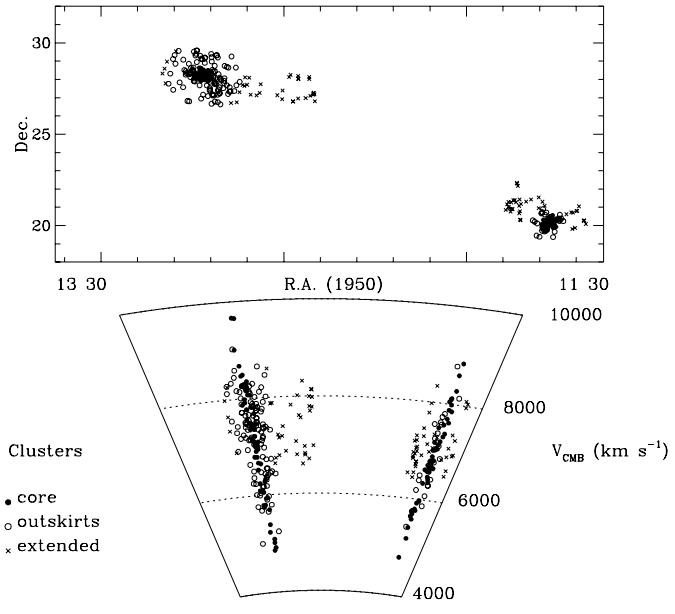

Fig. 7

Fig. 7. The distribution in celestial coordinates of galaxies belonging to the Coma and A 1367 clusters (Agg = 1–4), panel **a)**. A wedge diagram is given in panel **b)**

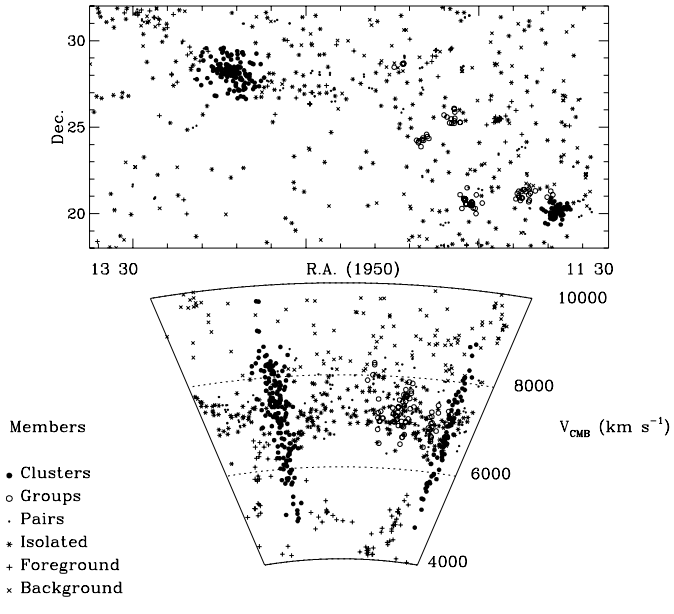

Fig. 8

Fig. 8. The distribution in celestial coordinates of members (Agg = 1–7) to the Coma–A 1367 supercluster, panel **a)**. A wedge diagram is given in panel **b)**

Column 11: the number of objects belonging to each aggregate.

5. Conclusions and summary

We obtained 117 new redshift measurements of GCGC galaxies, 102 of which in the direction of the Coma–A 1367 supercluster. With the new data, the total number of available redshifts in this direction of the sky is 1068 ($m_p \leq 15.7$).

The supercluster is centered at $\sim$7200 km s^{-1} and it extends from 6000 to 8500 km s^{-1}. It contains two rich clusters (Coma + A 1367) whose "fingers of God" stretch from 4000 to 10000 km s^{-1}.

By computing of the local galaxy density around each object, we separate galaxies belonging to five groups, from several multiplets and relatively isolated objects within the supercluster. This classification will be used to study the environmental dependence of properties of galaxies spanning over an order of magnitude in local density.

Acknowledgements. We wish to thank the TACS of the Loiano and Cananea telescopes for the generous amounts of time allocated to this project. G.G. wishes to thank the students of his course for their contribution during the observations and the data reduction. L.C. has had support from CONACYT (México) research grant No. 211290-5-1430PE.

References

de Lapparent V., Geller M., Huchra J., 1986, ApJ 302, L1
Gavazzi G., ApJ 320, 96
Gavazzi G., Randone I., Branchini E., 1995, ApJ 438, 590
Gavazzi G., Boselli A., 1996, Astroph. Lett. Comm. 35, 1
Giovanelli R., Haynes M., 1985, ApJ 292, 404
Gregory S., Thompson L., 1978, ApJ 222, 784
Huchra J., Geller M., de Lapparent L., Corwin H., 1990, ApJS 72, 433
Kogut A., et al., 1993, ApJ 419, 1
Nilson P., 1973, Uppsala Obs. Ann. 6 (UGC)
Tonry J., Davis M., 1979, AJ 84, 1511
Zabludoff A., Geller M., Huchra J., Ramella M., 1993, AJ 106, 1301
Zwicky F., Herzog E., Karpowicz M., Koval C., Wild P., 1961-1968, Catalogue of Galaxies and Clusters of Galaxies. Pasadena: Caltech (GCGC)